

Neutrino Constraints on Inelastic Dark Matter after CDMS II

Jing Shu ^{a,*}, Peng-fei Yin ^{b,†} and Shou-hua Zhu ^{b,‡}

^a*Institute for the Physics and Mathematics of the Universe,
The University of Tokyo, Chiba 277 – 8568, Japan*

^b*Institute of Theoretical Physics & State Key Laboratory of Nuclear Physics and Technology,
Peking University, Beijing 100871, P.R. China*

We discuss the neutrino constraints from solar and terrestrial dark matter (DM) annihilations in the inelastic dark matter (iDM) scenario after the recent CDMS II results. To reconcile the DAMA/LIBRA data with constraints from all other direct experiments, the iDM needs to be light ($m_\chi < 100$ GeV) and have a large DM-nucleon cross section ($\sigma_n \sim 10^{-4}$ pb in the spin-independent (SI) scattering and $\sigma_n \sim 10$ pb in the spin-dependent (SD) scattering). The dominant contribution to the iDM capture in the Sun is from scattering off Fe/Al in the SI/SD case. Current bounds from Super-Kamiokande exclude the hard DM annihilation channels, such as W^+W^- , ZZ , $t\bar{t}$ and $\tau^+\tau^-$. For soft channels such as $b\bar{b}$ and $c\bar{c}$, the limits are loose, but could be tested or further constrained by future IceCube plus DeepCore. For neutrino constraints from the DM annihilation in the Earth, due to the weaker gravitational effect of the Earth and inelastic capture condition, the constraint exists only for small mass splitting $\delta < 40$ keV and $m_\chi \sim (10, 50)$ GeV even in the $\tau^+\tau^-$ channel.

I. INTRODUCTION

A wide variety of cosmological observations, which include the highly precise measurements of the cosmic microwave background [1], galactic rotation curves [2], the weak gravitational lensing of distant galaxies by foreground structure [3], and the weak modulation of strong lensing around individual massive elliptical galaxies [4], all indicate that about 22% of our universe consists of non-baryonic, non-luminous dark matter (DM). The nature of DM, on the other hand, still remains a mystery.

The first direct detection experiment that provided strong evidence for dark matter is the DAMA collaboration, which announced an 8.3σ discovery [5] in the annual modulations of nuclear recoil rate. In the simplest DM models, such an event rate is excluded by two orders of magnitude in other low-background nuclear experiments. A widely invoked resolution of this controversy is the inelastic dark matter (iDM) model [6, 7], which introduces a transition to an excited state in the dark matter nucleus scattering. If the mass splitting δ is roughly 100 keV, which is close to the kinetic energy of a DM in the halo, the kinematics is significantly modified and the controversy can

be settled.

Very recently, the Cryogenic Dark Matter Search (CDMS II) announced the observation of two signal events ¹ with a 77% confidence level and additional two events just outside the signal region border [8]. Statistically this is not significant to claim a discovery, nevertheless, it is very suggestive if one believe such signals are coming from DM nuclei scattering. In particular, these two events with small recoil energies suggest that the mass of dark matter is smaller than 100 GeV ² with SI cross section $\sim O(10^{-8})$ pb which could escape other experimental constraints. Many models have been proposed since then [9]. In addition, limits on the dark matter nucleus cross section are obtained from the data. In the inelastic spin-independent (iSI) DM models, only a very narrow region of parameter space is allowed [8, 10–12], but the constraint can be large relaxed if one consider the inelastic spin-dependent (iSD) DM models [12].

Other experiments that give a strong constraint on the DM-nucleon cross section besides the di-

*Electronic address: jing.shu@ipmu.jp

†Electronic address: s7dx5v3@pku.edu.cn

‡Electronic address: aiwen.fan@pku.edu.cn

¹ CDMS has a very low background comparing to the other direct detection experiments and the two observed events are well separated from other events that have failed to pass the cuts. In other experiments, for instance XENON [10], many observed events are at the border of the cuts and are used to set limits on DM scattering cross section.

² Interestingly, the preferred DM mass region largely overlaps with the one used to explain DAMA in the iDM model.

rect detection experiments are the neutrino telescopes which are detecting the neutrino flux from DM captured and annihilated in the Sun or Earth. For example, Ref. [13] and Ref. [14, 15] give the neutrino constraints to the light elastic DM (eDM) and iSI DM which could account for DAMA results respectively. When the DM nucleus scattering is iSD, the constraints by the neutrino flux from the Sun can be dramatically different. The reason is that the kinetic energy requirement for a DM (χ) scattering inelastically with a nucleus (N) is

$$E_\chi > \delta \left(1 + \frac{m_\chi}{m_N} \right). \quad (1)$$

For light elements like hydrogen, only very energetic DM particles can scatter with them and get captured in the Sun if δ is not very small. Then the overall capture rate with their dominant contributions from light elements in the Sun will be significantly reduced. The modified kinematics for inelastic scattering in Eq. (1) also largely reduced the kinetic phase space of DM captured in the Earth because of the small escape velocity of the Earth. Therefore, it is of importance to perform a detailed analysis regarding the above issues motivated by the recent DAMA, CDMS results.

The paper is organized as follows. In Section II, we calculate the capture rate for both iSI and iSD DM in the Sun and we discuss the possible uncertainties in the calculation. In Section III, we obtain the constraint on the DM-nucleon inelastic cross section for different annihilation channels from Super-Kamiokande (Super-K) and the expected event number from the on-going large volume neutrino telescope, IceCube. In Section IV, we will discuss the neutrino constraint from iDM captured in the Earth. Finally we conclude and discuss our studies in Section V.

II. CAPTURE RATE FOR INELASTIC DARK MATTER IN THE SUN

When DM particles travel through the Sun system, they may get trapped by the gravitational potential and continue to lose energy with every collision against nucleus and captured in the Sun. The time evolution of the DM population in the Sun is given by the differential equation

$$\dot{N} = C_\odot - C_A N^2 - C_E N, \quad (2)$$

where C_\odot is the capture rate of the DMs in the Sun and annihilation rate is $\Gamma_A = C_A N^2 / 2$ with

$C_A = \langle \sigma v \rangle / V_{\odot eff}$, C_E is the inverse time for DM to escape via evaporation which will be neglected below since our DM is not very light. For typical DM we have considered, the time scale required to reach equilibrium between capture and annihilation, $t_{eq} = 1 / \sqrt{C_\odot C_A}$, is much smaller than the age of the solar system so the annihilation rate is saturated at half of the capture rate $\Gamma_A = C_\odot / 2$. Therefore, calculating the DM capture rate in the Sun is crucial to estimate the final neutrino flux from the Sun [14–18].

Suppose a DM particle has a velocity u very far away from the Sun, at some point the escape velocity in a shell is $v(r)$, the DM velocity w will be

$$w^2 = u^2 + v(r)^2. \quad (3)$$

In the DM-nucleus center of mass frame, it is easy to see that in order to have a DM-nucleus inelastic scattering, the following condition is required

$$\frac{\mu w^2}{2} > \delta, \quad (4)$$

where $\mu \equiv m_\chi m_N / (m_\chi + m_N)$ is the DM-nucleus reduced mass, δ is the mass split between two DM states. The escape velocity $v(r)$ is approximated as [19]

$$v^2(r) = v_c^2 - \frac{M(r)}{M_\odot} (v_c^2 - v_s^2), \quad (5)$$

where M_\odot is the mass of the Sun and $v_c = 1354$ km/s and $v_s = 795$ km/s. $M(r)$ is the mass profile of the Sun which can be obtained by the Sun density profile [20]

$$\rho(r) = \rho_0 \exp(-B \frac{r}{R_\odot}), \quad (6)$$

where $\rho_0 = 236.93$ g/cm³ and $B = 10.098$.

The DM capture rate in the Sun is given by

$$C_\odot = \int 4\pi r^2 dr \int du \frac{f(u)}{u} w \Omega(w), \quad (7)$$

where $f(u)$ is the DM velocity distribution at infinity, $\Omega(w)$ is the rate per unit time that a DM with velocity w scatter to a velocity less than v . We assume the DM velocity distribution far from the Sun follows a Maxwell-Boltzmann distribution in the Sun rest frame

$$f(x)dx = \frac{\rho_\chi}{m_\chi} \frac{4}{\sqrt{\pi}} x^2 e^{-x^2} e^{-\eta^2} \frac{\sinh(2x\eta)}{2x\eta} dx \quad (8)$$

where the dimensionless variables are defined as $x^2 \equiv u^2/v_0^2$ and $\eta^2 \equiv v_\odot^2/v_0^2$, $v_0 = 220$ km/s is the average local circular velocity which is related to DM velocity dispersion \bar{v} as $v_0^2/\bar{v}^2 = 2/3$.

Taking into account the form factor suppression, the scattering function $\Omega(w)$ is given by

$$\begin{aligned}\Omega(w) &= \sum_i \frac{n_i w}{Q_{i\ max} - Q_{i\ min}} \int_{Q'_{i\ min}}^{Q_{i\ max}} dQ_i \\ &\times (\sigma_i^{SI} F_i^2(Q_i) + \sigma_i^{SD} S_i(Q_i))\end{aligned}\quad (9)$$

where i denotes each species of nuclei in the Sun and we will omit it below, n is the number density of the nuclei, Q is the energy transfer in the scattering, $Q_{max}(Q_{min})$ denotes the possible maximum(minimum) energy transfer and Q_{cap} is the minimal energy transfer which requires DM could be captured only with a velocity less than v , and we define lower limit of integration as $Q'_{min} = \max(Q_{cap}, Q_{min})$. These energy transfer functions are given by [14]

$$\begin{aligned}Q_{max} &= \frac{1}{2} m_\chi w^2 \left\{ 1 - \frac{\mu^2}{m_N^2} \right. \\ &\times \left. \left(1 - \frac{m_N}{m_\chi} \sqrt{1 - \frac{\delta}{\mu w^2/2}} \right)^2 \right\} - \delta\end{aligned}\quad (10)$$

$$\begin{aligned}Q_{min} &= \frac{1}{2} m_\chi w^2 \left\{ 1 - \frac{\mu^2}{m_N^2} \right. \\ &\times \left. \left(1 + \frac{m_N}{m_\chi} \sqrt{1 - \frac{\delta}{\mu w^2/2}} \right)^2 \right\} - \delta\end{aligned}\quad (11)$$

$$Q_{cap} = \frac{1}{2} m_\chi (w^2 - v^2) - \delta, \quad (12)$$

and one has to impose the condition

$$Q_{max} > Q_{cap} \quad (13)$$

for the capture to happen. $\sigma^{SI(SD)}$ is the inelastic SI (SD) cross section and $F(Q)$ is the SI form factor. The term $\sigma^{SD} S(Q)$ will be decomposed into SD cross sections and SD form factors for different spin J later. The inelastic SI (SD) cross section is given by

$$\begin{aligned}\sigma^{SI} &= \sqrt{1 - \frac{\delta}{\mu w^2/2}} \left(\frac{\mu}{\mu_{\chi n}} \right)^2 \\ &\times \left(\frac{f_p Z + f_n (A - Z)}{f_p} \right)^2 \sigma_n^{SI}\end{aligned}\quad (14)$$

where A is the atomic mass number, Z is the charge of the nucleus, $\mu_{\chi n} \equiv m_\chi m_n / (m_\chi + m_n)$ is the DM-nucleon reduced mass, $f_p(f_n)$ is the SI DM coupling to protons (neutrons) and we normalize it to $f_p = f_n$, σ_n^{SI} is the DM-nucleon SI scattering cross section. We can see that if $f_p \simeq f_n$, the DM-nuclei SI cross section is proportional to A^2 . Moreover, if $m_\chi \gg m_N$, the reduced mass μ/m_N will provide another enhancement factor of A^2 . We can expect heavy nuclei with large abundance in the Sun, such as Fe, to play a more important role in the capture process. For the SI form factor, we use the Helm form factor as,

$$F(Q) = 3e^{-k^2 s^2/2} \frac{\sin(kr) - kr \cos(kr)}{(kr)^3}, \quad (15)$$

with nuclear skin thickness $s = 1$ fm, effective nuclear radius $r = \sqrt{R^2 - 5s^2}$, $R = 1.2A^{1/3}$ fm, and momentum transfer $k = \sqrt{2m_N Q}$.

The SD cross section with form factor for spin-non-zero nuclei is

$$\begin{aligned}\sigma^{SD} S(Q) &= \frac{4\pi}{3a_p^2(2J+1)} \sqrt{1 - \frac{\delta}{\mu w^2/2}} \left(\frac{\mu}{\mu_{\chi n}} \right)^2 \\ &\times (a_0^2 S_{00}(k) + a_0 a_1 S_{01}(k) + a_1^2 S_{11}(k)) \sigma_n^{SD},\end{aligned}\quad (16)$$

where $a_0 = a_p + a_n$ and $a_1 = a_p - a_n$ are isoscalar spin and isovector spin couplings, a_p and a_n are the effective spin DM-proton and DM-neutron couplings which we assume $a_p = 1$ and $a_n = 0$ in the below, $S_{00}(k), S_{01}(k), S_{11}(k)$ are nuclear structure functions. In many nuclei models, the nuclear spin is carried by the unpaired nucleons. Therefore we focus on the nuclei with an odd nucleon number in the SD scattering process. In the calculation we use the nuclear structure functions provided by Ref. [21].

The capture rate of 50 GeV DM due to different species of nuclei in the Sun as a function of the mass splitting δ is calculated for both iSI and iSD DM. The results depend on some astrophysical parameters and as a reference point, we choose $\rho_\chi = 0.3$ GeV cm $^{-3}$, $v_\odot = 220$ km/s and $v_0 = 220$ km/s in the Maxwell-Boltzmann distribution. The element abundances are given by Ref. [22] in the form of $\epsilon_i = \log(n_i/n_H) + 12$ and the mass fraction of hydrogen (helium) is 0.7381 (0.2485). In the calculation for SI capture, we pick out the species with $\epsilon_i > 6$. For SD capture, we calculate ${}^1\text{H}$, ${}^{19}\text{F}$, ${}^{23}\text{Na}$, ${}^{27}\text{Al}$, ${}^{29}\text{Si}$ and ${}^{39}\text{K}$. As we can see in FIG. 1 and 2, Fe and Al provide most contributions to the iSI and iSD scattering processes respectively and

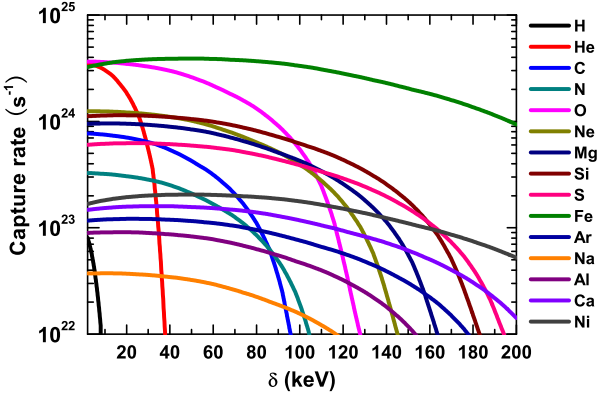


FIG. 1: Capture rate of 50 GeV spin-independent iDM with DM-nucleon cross section of $\sigma_n^{SI} \sim 10^{-4}$ pb as a function of the mass splitting δ due to different species of nuclei in the Sun. We choose $\rho_\chi = 0.3$ GeV cm $^{-3}$, $v_\odot = 220$ km/s and $v_0 = 220$ km/s in the Maxwell-Boltzmann distribution.

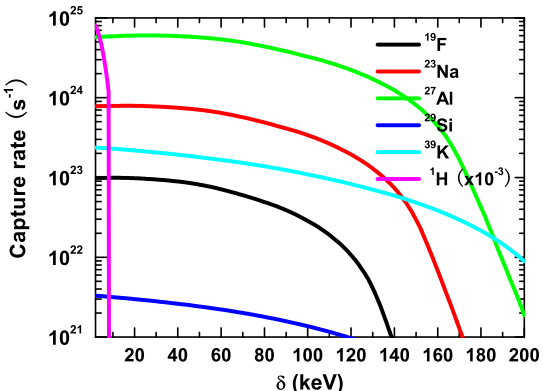


FIG. 2: Capture rate of 50 GeV spin-dependent iDM with $\sigma_n^{SD} \sim 10$ pb as a function of the mass splitting δ due to different species of nuclei in the Sun.

one can safely neglect the Hydrogen contribution in the iSD scattering for $\delta > 10$ keV. The capture rate is always sensitive to the abundance of heavy nuclei.

Finally, we give some short comments on the possible uncertainty in the calculation for solar DM capture rate. The input astrophysics parameters are the local DM mass density ρ_χ , velocity of the Sun v_\odot , average local circular velocity v_0 , and solar elemental abundances ϵ_i . The capture rate is proportional to ρ_χ and the results will increase if a larger local DM mass density is available [23] or the solar system is passing through DM sub-

structure [24]. We also assume the DM infinity velocity distribution is a Maxwell-Boltzmann distribution which depends on parameters v_\odot and v_0 . As discussed in Ref. [15], if these two parameters vary in the region of 200 km/s $< v_\odot, v_0 < 300$ km/s, the capture rate will be changed by a factor less than two. One should also notice that, if the velocity distribution deviates from an ordinary Maxwell-Boltzmann distribution, the result will also be changed. In our discussions, for simplicity, we assume the solar chemical composition does not change in the Sun. The capture rate is sensitive to the abundance of heavy nuclei and increasing the number density of heavy nuclei in the center of the Sun will increase the overall capture rate by a few [15]. There are also uncertainties arising from the nuclear form factor. For the SI scattering, the Helm form factor we used in the calculation is less accurate at large momentum transfers and might be improved by using some more precise form factors [25]. For the SD scattering, the nuclear structure functions in Ref. [21] are only considered for direct DM search on the Earth, so the q_{max} used in the finite momentum transfer approximation may not be large enough for DM-nucleus scattering in the Sun if our DM is heavy.

III. LIMITS FROM THE NEUTRINO TELESCOPES

If the DM capture and annihilation processes reach equilibrium, we can simply get the DM annihilation rate

$$\Gamma_A = C_\odot / 2 \quad (17)$$

The different DM annihilation channels give different initial neutrino spectra [26]. If the DM annihilates to e^+e^- or $\mu^+\mu^-$, they will not contribute to neutrino signals. This is because for muons, they always lose most of their energy before decaying in the center of the Sun. For annihilation channel to $\tau^+\tau^-$, the neutrinos are induced by τ leptonic decays $\tau \rightarrow \mu\nu\nu$, $e\nu\nu$, and hadronic decays such as $\tau \rightarrow \pi\nu$, $K\nu$, $\pi\pi\nu$ et al. For the heavy final annihilation states W^+W^- , ZZ , $t\bar{t}$, they produce neutrinos via cascade decays and the neutrino spectra for such channels are hard. For quark channels, the hadronization process produces mesons and baryons, and then induces neutrinos via hadron decays. The neutrino spectra for such channels are soft. Notice that the light mesons easily lose their energy before decays, so

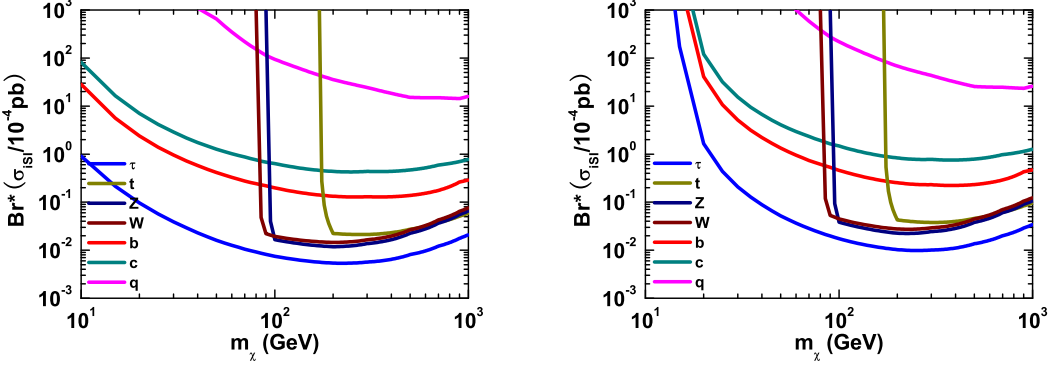


FIG. 3: Super-K solar neutrino limits on the cross section per nucleon times the branching ratio to different annihilation channels for the iSI DM with mass splitting $\delta = 40$ keV (left) and $\delta = 130$ keV (right). We show the limits on seven annihilation channels including $\tau\bar{\tau}$, $t\bar{t}$, W^+W^- , ZZ , $b\bar{b}$, $c\bar{c}$ and $q\bar{q}$ (q denotes light quark here).

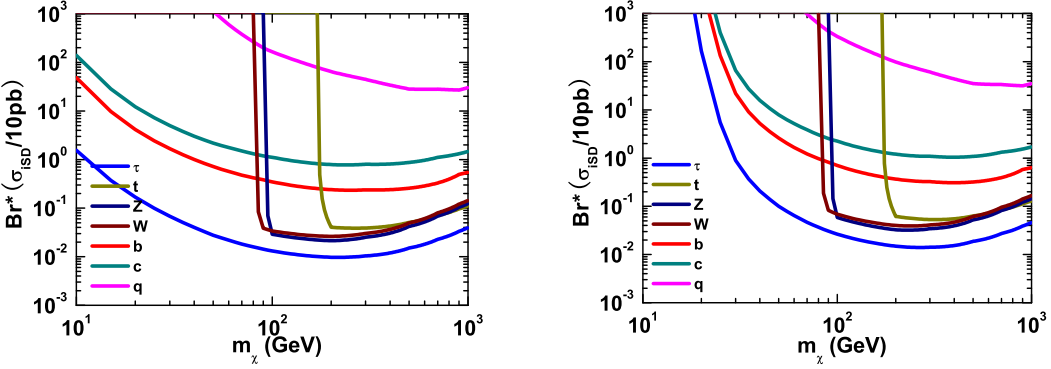


FIG. 4: Super-K solar neutrino limits on the cross section per nucleon times the branching ratio to different annihilation channels for the iSD DM with mass splitting $\delta = 40$ keV (left) and $\delta = 130$ keV (right).

the contributions to the neutrino signals from light quarks are usually small.

The neutrinos produced at the solar center will interact with the matter in the Sun. These effects include the neutral current (NC) interaction, the charged current (CC) interaction, and tau neutrino ν_τ reinjection from secondary tau decays. The neutrino oscillations including the vacuum mixing and the MSW matter effects are also important. Here we use the results given by Ref. [26] to take into account the above effects during the neutrinos' propagation. The differential neutrino flux at the Earth

is

$$\frac{dN_\nu}{dE_\nu} = \frac{\Gamma_A}{4\pi R_{SE}^2} \sum_i Br_i \left(\frac{dN_\nu}{dE_\nu} \right)_i \quad (18)$$

where i runs over the different DM annihilation channels with branching ratios Br_i , dN_ν/dE_ν is the neutrino spectrum at the Earth after propagation, and R_{SE} is the Sun-Earth distance.

We can calculate the muon rate at the detector

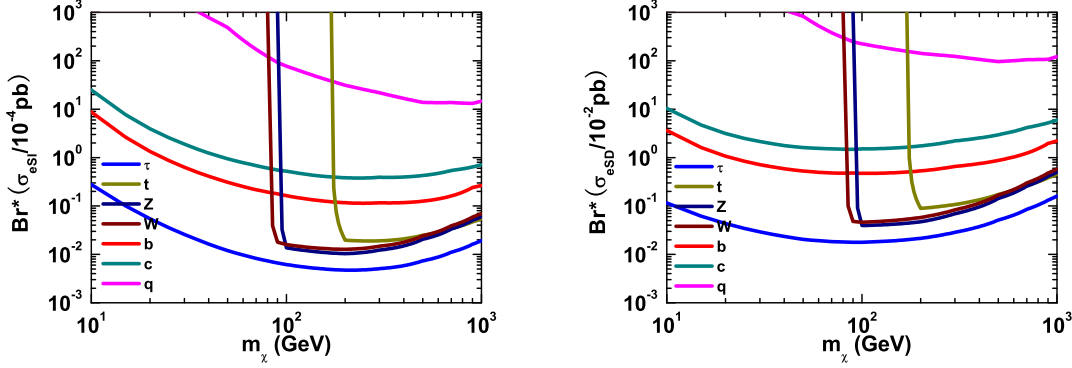


FIG. 5: Super-K solar neutrino limits on the cross section per nucleon times the branching ratio to different annihilation channels for the elastic spin-independent (eSI) DM (left) and elastic spin-dependent (eSD) DM (right).

as³

$$\frac{d\phi_\mu}{dE_\mu} = \int_{E_{th}}^{m_\chi} dE_{\nu_\mu} \frac{dN_{\nu_\mu}}{dE_{\nu_\mu}} \left[\frac{d\sigma_{\text{CC}}^{\nu p}(E_{\nu_\mu}, E_\mu)}{dE_\mu} n_p + (p \rightarrow n) R(E_\mu) + (\nu \rightarrow \bar{\nu}) \right] \quad (19)$$

where n_p (n_n) is the number density of protons (neutrons) in matter around the detector, the muon range $R(E_\mu)$ is the distance that a muon could travel in matter before its energy drops below the detector's threshold energy E_{th} which is given by

$$R(E_\mu) = \frac{1}{\rho\beta} \ln \left(\frac{\alpha + \beta E_\mu}{\alpha + \beta E_{th}} \right), \quad (20)$$

with α, β the parameters describing the energy loss of muons in matter.

The cross sections of deep inelastic neutrino-nucleon scattering processes are given by [28]

$$\frac{d\sigma_{\text{CC/NC}}^{\nu p,n}(E_\nu, y)}{dy} \simeq \frac{2 m_{p,n} G_F^2}{\pi} E_\nu \times \left(a_{\text{CC/NC}}^{\nu p,n} + b_{\text{CC/NC}}^{\nu p,n} (1-y)^2 \right), \quad (21)$$

where $y \equiv 1 - E_\ell/E_\nu$. We can see that the neutrino detector is more powerful to observe neutrino signals in the high energy region. Because the

neutrino-nucleon cross section and muon range increase as E_ν , while the atmospheric neutrino background decrease as E_ν^3 .

To obtain limits on the cross section per nucleon times the branching ratio $\sigma_n \cdot \text{Br}_i$, we use the upper bound on high energy up-going muon flux in the direction of Sun given by Super-K group [29]. The Super-K detector is located in a mine with 1000 m rock overburden which contains 50,000 ton water. The detector can detect up-going muons with measured path length of at least 7 m which is equivalent to the detector energy threshold 1.6 GeV. So the Super-K detector has a wide detecting range for high energy neutrino. Super-K group analyzed the data in 1679.6 days of detector live time, and no events induced by DM annihilation/decay are confirmed in the directions of the Sun, the center of Earth, and the Galactic Center. A stringent limit for up-going muon flux $O(10^{-15}) \text{ cm}^{-2} \text{ s}^{-1}$ constrains the DM model. Here we use the constraint in Ref. [29] for all annihilation channels.

The Super-K limits on $\sigma_n \cdot \text{Br}_i$ to different annihilation channels for iSI and iSD DM with different mass splitting δ are presented in FIG. 3, and 4 respectively. For a typical DM annihilation cross section of 10^{-4} pb (or higher) that explains DAMA in the iSI DM case, the limits are quite constraining on hard channels (W^+W^- , ZZ , $t\bar{t}$, $\tau^+\tau^-$), are lessened in softer channels like $c\bar{c}$ and $b\bar{b}$ and are quite loose in the light quark channels. In the iSD DM case, the typical DM annihilation cross section (or higher) to explain DAMA is enhanced to 10 pb [12]. Interestingly, even though

³ A different formula that accounts for the energy dependent muon flux can be found in Ref. [27].

the cross section is 10^5 times higher than the iSI DM case, we reach a similar conclusion that the limits are quite constraining on hard channels, are lessened in softer channels like $c\bar{c}$ and $b\bar{b}$ and are quite loose in the light quark channels. In order to see how the inelastic property of DM nucleus scattering changes the limits, we also calculate the Super-K limits on $\sigma_n \cdot Br_i$ to different annihilation channels for eDM. In the SI case, making the scattering inelastic changes the results at most an order of magnitude for reasonable δ . In the SD case, however, the limit is loosened by 3 orders of magnitude when hydrogen no longer contributes to the dark matter capture in the Sun.

The on-going large volume neutrino telescopes, such as IceCube and KM3NET, are more powerful to probe high energy neutrinos. IceCube located between depth of 1.45 km and 2.45 km in the south pole will have an effective detecting area of 1 km^2 . In 2007, IceCube consisted of 22 strings has provided a more stringent upper limit to muon flux from the Sun [30]. The main shortcoming of IceCube 22-strings is its high energy threshold. So the experimental results are only useful to constrain the heavy DM⁴. The complete detector consisted of 80 strings might reduce the energy threshold to 50 GeV. We need to notice that the effective detecting area of IceCube decreases rapidly in the low energy region. In addition, the angular resolution becomes worse in such energy region. So the capability of IceCube to search for light DM is weaker than that for heavy DM.

But it is worth remarking, additional IceCube 6 special strings named DeepCore, are powerful to improve the capability of the detector and reduce the detection threshold down to 10 GeV [31, 32]. In the FIG. 6, we show the total number of events at the IceCube plus DeepCore. Here we use the effective neutrino detection area of IceCube plus DeepCore given by Ref. [32] to calculate the event rate at the detector. The number of background events from atmospheric neutrinos within a 3° window is estimated ~ 50 in the energy range $E \sim (10, 200)$ GeV. For heavy iDM $m_\chi > 100$ GeV, the IceCube plus DeepCore is very powerful to test most of the iDM annihilation channels, which include all hard

channels and soft channels to $b\bar{b}$ and $c\bar{c}$. For the iDM lighter than 100 GeV, comparing with FIG. 3 and 4 based on the Super-K 90% C.L. exclusion limit, we can see that the IceCube plus DeepCore also has capability to test or further constrain the iDM model with soft annihilation channels to $b\bar{b}$ and $c\bar{c}$.

IV. NEUTRINO CONSTRAINT FROM TERRESTRIAL INELASTIC DARK MATTER ANNIHILATIONS

Unlike the Sun, the main constituents of the Earth are heavy nuclei, such as O, Al, Si, Mg, Fe and Ni. Since the abundances of Fe and Al are 31.9% and 1.59% respectively, we expect that the abundance of such heavy elements helps the capture process. Nevertheless, probing neutrino signals from terrestrial iDM annihilations is more difficult than probing them from solar iDM annihilations. There are two main reasons for this. First, as a gravitational system, the Earth is far smaller than the Sun with a rather small escape velocity, so it is more difficult to trap DM in the center of the Earth. In the iDM scenario, the situation becomes even worse due to the kinetic suppression induced by inelastic capture condition. Second, it is well known that terrestrial DM capture and annihilation processes can not reach equilibrium in the ordinary DM scenario, so the annihilation rate of DM trapped in the Earth is even smaller than half of the capture rate.

Now we turn to Eq. (4) and (13) and see the first reason of suppression explicitly. We can rewrite Eq. (13) as

$$\frac{\chi'}{\chi'^2_-} > \frac{u^2}{v^2} \quad (22)$$

where we use a similar notation as Ref. [16]

$$\chi \equiv \frac{m_\chi}{m_N}, \quad s \equiv \sqrt{1 - 2\delta/(\mu w^2)}, \quad (23)$$

and

$$\chi'_- \equiv \frac{\chi - s}{2}, \quad \chi' \equiv \chi \left(\frac{1+s}{2} \right) + \frac{1-s^2}{4}. \quad (24)$$

The escape velocity of the Earth $v \simeq 10 \text{ km/s}$ is very small compared to the escape velocity of the Sun $\simeq 10^3 \text{ km/s}$ and the velocity dispersion of local DM $u \sim \bar{v} \simeq 270 \text{ km/s}$, so the right hand side of the

⁴ For the $b\bar{b}$ and W^+W^- channels, the constraints are available for DM heavier than 250 GeV and 500 GeV respectively. For the constraints to iDM, one can see the Ref. [15].

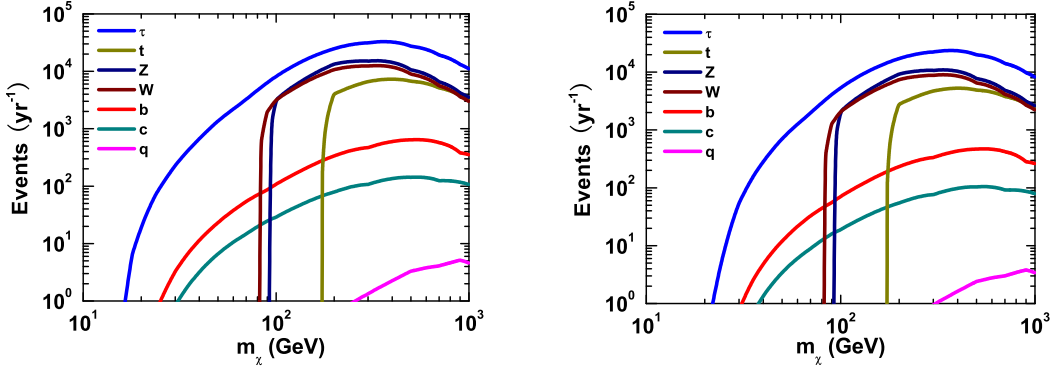


FIG. 6: (left) Neutrino event number in one year at IceCube (with DeepCore) for the iSI DM with $\sigma_n^{SI} = 10^{-4}$ pb (left) and iSD DM with $\sigma_n^{SD} = 10$ pb (right). We choose mass splitting $\delta = 130$ GeV here.

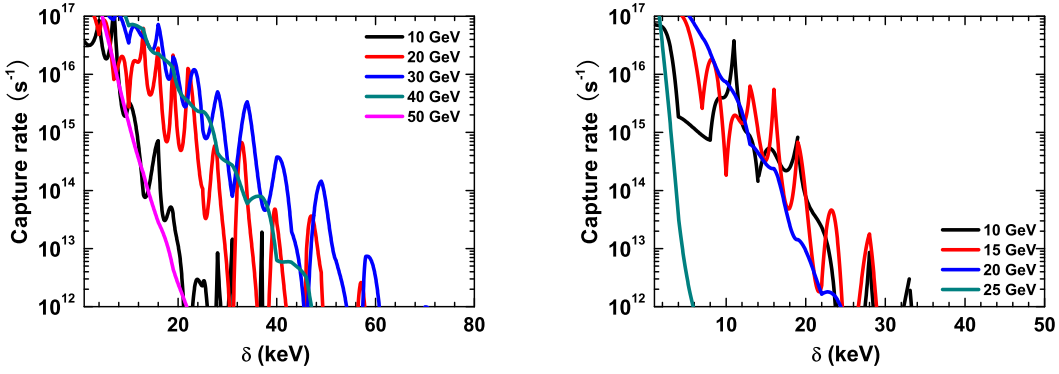


FIG. 7: Terrestrial iDM capture rate for the iSI DM with $\sigma_n^{SI} = 10^{-4}$ pb (left) and iSD DM with $\sigma_n^{SD} = 10$ pb (right).

capture condition Eq. (22) is a large value. When the mass of DM is comparable to or larger than that of a nucleus, such as Fe or Al, the left hand side of Eq. (22) is suppressed by m_χ so it is difficult to satisfy the capture condition. If the DM is much lighter than the nuclei, the condition Eq. (22) is still not easy to satisfy. Moreover it is difficult to satisfy the inelastic scattering condition Eq. (4) simultaneously. So the most promising situation is that DM and nuclei have similar masses and δ must not be large.

The terrestrial iDM capture and annihilation do

not reach equilibrium in ordinary DM scenario⁵. Following from Eq. (2), the DM annihilation rate is

$$\Gamma_A = \frac{C_\oplus}{2} \tanh^2(t_\oplus/t_{eq}), \quad (25)$$

where t_\oplus is the age of Earth, C_\oplus is the capture rate of the DMs in the Earth. The equilibrium time, effective annihilation rate is defined as $t_{eq} \equiv$

⁵ If the DM annihilation cross section is far larger than ordinary value $3 \times 10^{-26} \text{ cm}^3/\text{s}$ due to some enhancements such as Sommerfeld effect, the terrestrial DM capture and annihilation could reach equilibrium [34].

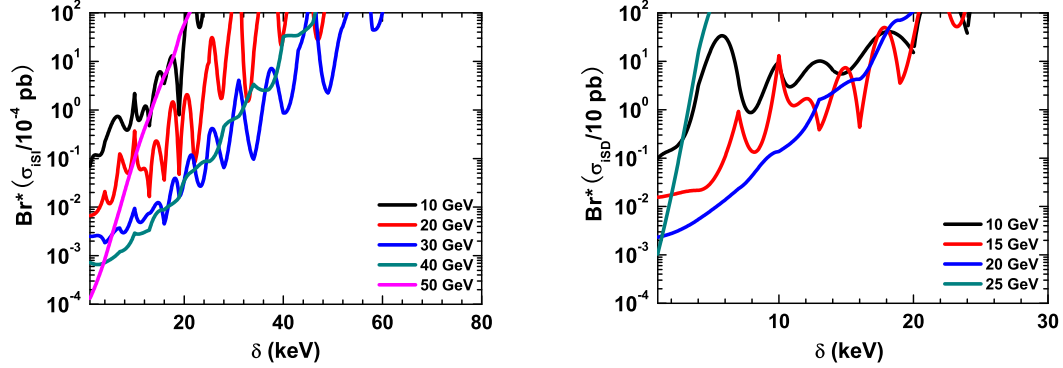


FIG. 8: Super-K terrestrial neutrino limits on the cross section per nucleon times the branching ratio to different annihilation channels for the iSI DM (left) and iSD DM (right).

$1/\sqrt{C_{\oplus} C_A}$, $C_A \equiv \langle \sigma v \rangle / V_{\oplus eff}$ respectively. It is also useful to define a critical capture rate for the Earth as $C_{\oplus}^c \equiv 1/C_A t_{\oplus}^2 \sim 10^{14} s^{-1} (\text{TeV}/m_{\chi})^{3/2}$. If $C_{\oplus} > C_{\oplus}^c$, the DM capture and annihilation in the Earth could reach equilibrium.

It is straightforward to get numerical results by using the method in Sec II. Here we use the mass density profile and the composition of the Earth provided by Ref. [20] and [33] respectively. For simplicity, we assume the Earth is in free space [16]. If the gravitational interaction of the Sun is taken into account, there is a correction factor of $O(1)$ [35] to the capture rate. In FIG. 7, we show the results of terrestrial iDM capture rate for SI and SD scattering processes. We find that for very heavy or light DM, the capture process is highly suppressed. So we only give the capture rate for the iDM with typical mass in the range of (10, 50) GeV which is similar to the mass of nuclei of interest. It is interesting to notice that there are surges as δ is varying. The peaks of these surges ($\chi'_- \rightarrow 0$) are quite similar to the “resonant enhancement” in the eDM case when DM mass reaches to the nuclei’s mass as discussed in Ref. [16] and is absent if the DM is not light enough. For the iDM scenario, we need to notice that for the n species of nuclei of interest here, there are $2n$ inelastic capture conditions to be satisfied or obeyed. So if the mass of DM is similar to that of the nuclei, the terrestrial capture rate is very sensitive to the parameters of m_N , m_{χ} and δ .

Here we use the upper limit for up-going muon flux from the center of the Earth provided by Super-K [29] to constrain the iDM model. We

only show the most stringent constraints assuming all the DM annihilation products are $\tau^+ \tau^-$. We can see the results in FIG. 8 and we find that the constraints from Earth-born neutrinos are weaker than those from the Sun. The most stringent constraints arise from small δ and $m_{\chi} \sim (10, 50)$ GeV.

V. CONCLUSION AND DISCUSSION

Inelastic dark matter (iDM) is an excellent candidate to explain the DAMA annual modulation result. Recently, the CDMS II announced the observation of two signal events and set a more stringent constraint to the iDM model to account for DAMA results. The mass of the iDM is not heavier than 100 GeV and the DM-nucleon cross section is typically 10^{-4} pb (or higher) for iSI case and is 10 pb (or higher) for iSD case.

In this work, we discuss the constraints by neutrino signals from solar and terrestrial iDM annihilations motivated after DAMA and CDMS II results. The neutrino flux from the Sun or Earth depends on the capture rate and the constraint on DM-nucleon cross section is quite different from the eDM case. For iSI/iSD scattering, the main contribution to the capture rate in the Sun is from Fe/Al and in the latter case, the capture from H is highly kinematically suppressed. Although the types of nuclei that contribute to the capture rate are quite different in iSI and iSD DM models, the constraints for the iDM annihilation channels for the typical DM-nucleon cross section are actually similar. The Super-K null results set very

stringent constraints to the hard DM annihilation channels such as W^+W^- , ZZ , $t\bar{t}$ and $\tau^+\tau^-$. For the soft channels such as $b\bar{b}$ and $c\bar{c}$, the limits are loose. With the IceCube 80-strings plus DeepCore, it can discover or exclude such channels. If the DM annihilation products are light charged leptons e^+e^- , $\mu^+\mu^-$, light mesons or some new light bosons, there are no constraints from the neutrino detection. For neutrinos from DM annihilation in the Earth, the constraint is weaker than the one in the Sun. This is mainly due to the fact that Earth being a small gravitational system that captures the DM. Moreover, the terrestrial iDM capture rate is suppressed due to the inelastic capture condition. Furthermore, the terrestrial iDM capture and annihilation do not reach equilibrium in most of its parameter space. The constraint is available only for small δ and iDM with mass of several tens of GeV where similar behaviors as the “resonance enhancement” in the eDM case occur.

If the DAMA and CDMS II results are really induced by DM, we could expect the XENON 100 [36] or other direct detection experiments to give the similar observations in the immediate future. Nevertheless, the constraints and future detection

prospects we have obtained from neutrino telescope should be considered in any explanations based on iDM. Other on-going indirect detection experiments and the Large Hadron Collider also have the capability to detect the DM signals. It is exciting and useful to think about all these experiments and achieve a complete picture of DM.

VI. ACKNOWLEDGEMENT

We would like to thank Paul H. Frampton, Sourav Mandal and Matthew Sudano for useful discussions. The work of J.S. was supported by the World Premier International Research Center Initiative (WPI initiative) MEXT, Japan and Grant-in-Aid for scientific research (Young Scientists (B) 21740169) from Japan Society for Promotion of Science (JSPS). The work of P.F.Y. and S.H.Z was supported by the Natural Sciences Foundation of China (Nos. 10775001, 10635030). P.F.Y. would like to acknowledge the hospitality of Institute for Physics and Mathematics of the Universe (IPMU) while the work was initiated.

-
- [1] E. Komatsu *et al.* [WMAP Collaboration], *Astrophys. J. Suppl.* **180**, 330 (2009) [arXiv:0803.0547 [astro-ph]].
 - [2] A. Borriello and P. Salucci, *Mon. Not. Roy. Astron. Soc.* **323**, 285 (2001).
 - [3] H. Hoekstra, H. Yee and M. Gladders, *New Astron. Rev.* **46**, 767 (2002).
 - [4] R. B. Metcalf, L. A. Moustakas, A. J. Bunker and I. R. Parry, *Astrophys. J.* **607**, 43 (2004); L. A. Moustakas and R. B. Metcalf, *Mon. Not. Roy. Astron. Soc.* **339**, 607 (2003)
 - [5] R. Bernabei *et al.* [DAMA Collaboration], *Eur. Phys. J. C* **56**, 333 (2008) [arXiv:0804.2741 [astro-ph]].
 - [6] D. Tucker-Smith and N. Weiner, *Phys. Rev. D* **64**, 043502 (2001) [arXiv:hep-ph/0101138].
 - [7] S. Chang, G. D. Kribs, D. Tucker-Smith and N. Weiner, *Phys. Rev. D* **79**, 043513 (2009) [arXiv:0807.2250 [hep-ph]].
 - [8] Z. Ahmed *et al.* [The CDMS-II Collaboration and CDMS-II Collaboration], arXiv:0912.3592 [astro-ph.CO].
 - [9] M. Kadastik, K. Kannike, A. Racioppi and M. Raidal, arXiv:0912.3797 [hep-ph]; N. Bernal and A. Goudelis, arXiv:0912.3905 [hep-ph]; A. Bottino, F. Donato, N. Fornengo and S. Scopel, arXiv:0912.4025 [hep-ph]. D. Feldman, Z. Liu and P. Nath, arXiv:0912.4217 [hep-ph]; M. Ibe and T. T. Yanagida, arXiv:0912.4221 [hep-ph]; R. Allahverdi, B. Dutta and Y. Santoso, arXiv:0912.4329 [hep-ph]; M. Endo, S. Shirai and K. Yonekura, arXiv:0912.4484 [hep-ph]; Q. H. Cao, I. Low and G. Shaughnessy, arXiv:0912.4510 [hep-ph]; Q. H. Cao, C. R. Chen, C. S. Li and H. Zhang, arXiv:0912.4511 [hep-ph]; K. Cheung and T. C. Yuan, arXiv:0912.4599 [hep-ph]; J. Hisano, K. Nakayama and M. Yamanaka, arXiv:0912.4701 [hep-ph]; X. G. He, T. Li, X. Q. Li, J. Tandean and H. C. Tsai, arXiv:0912.4722 [hep-ph]; I. Gogoladze, R. Khalid, S. Raza and Q. Shafi, arXiv:0912.5411 [hep-ph]; M. Aoki, S. Kanemura and O. Seto, arXiv:0912.5536 [hep-ph]; R. Foot, arXiv:1001.0096 [hep-ph]. M. Asano and R. Kitano, arXiv:1001.0486 [hep-ph]. W. S. Cho, J. H. Huh, I. W. Kim, J. E. Kim and B. Kyae, arXiv:1001.0579 [hep-ph].
 - [10] J. Angle *et al.* [XENON Collaboration], *Phys. Rev. Lett.* **100**, 021303 (2008) [arXiv:0706.0039 [astro-ph]].
 - [11] K. Schmidt-Hoberg and M. W. Winkler, *JCAP* **0909**, 010 (2009) [arXiv:0907.3940 [astro-ph.CO]].

- [12] J. Kopp, T. Schwetz and J. Zupan, arXiv:0912.4264 [hep-ph].
- [13] D. Hooper, F. Petriello, K. M. Zurek and M. Kamionkowski, Phys. Rev. D **79**, 015010 (2009) [arXiv:0808.2464 [hep-ph]].
- [14] S. Nussinov, L. T. Wang and I. Yavin, JCAP **0908**, 037 (2009) [arXiv:0905.1333 [hep-ph]].
- [15] A. Menon, R. Morris, A. Pierce and N. Weiner, arXiv:0905.1847 [hep-ph].
- [16] A. Gould, Astrophys. J. **321**, 571 (1987).
- [17] G. Jungman, M. Kamionkowski and K. Griest, Phys. Rept. **267**, 195 (1996) [arXiv:hep-ph/9506380].
- [18] G. Wikstrom and J. Edsjo, JCAP **0904**, 009 (2009) [arXiv:0903.2986 [astro-ph.CO]].
- [19] A. Gould, Astrophys. J. **388**, 338 (1992).
- [20] R. Gandhi, C. Quigg, M. H. Reno and I. Sarcevic, Astropart. Phys. **5**, 81 (1996) [arXiv:hep-ph/9512364].
- [21] V. A. Bednyakov and F. Simkovic, Phys. Part. Nucl. **37**, S106 (2006) [arXiv:hep-ph/0608097].
- [22] M. Asplund, N. Grevesse, A. J. Sauval and P. Scott, Ann. Rev. Astron. Astrophys. **47**, 481 (2009) [arXiv:0909.0948 [astro-ph.SR]].
- [23] T. Bruch, A. H. G. Peter, J. Read, L. Baudis and G. Lake, Phys. Lett. B **674**, 250 (2009) [arXiv:0902.4001 [astro-ph.HE]].
- [24] S. M. Koushiappas and M. Kamionkowski, Phys. Rev. Lett. **103**, 121301 (2009) [arXiv:0907.4778 [astro-ph.CO]].
- [25] G. Duda, A. Kemper and P. Gondolo, JCAP **0704**, 012 (2007) [arXiv:hep-ph/0608035].
- [26] M. Cirelli, N. Fornengo, T. Montaruli, I. Sokalski, A. Strumia and F. Vissani, Nucl. Phys. B **727**, 99 (2005) [Erratum-ibid. B **790**, 338 (2008)] [arXiv:hep-ph/0506298].
- Web pages:
www.to.infn.it/~fornengo/DMnu.html,
www.cern.ch/astrumia/DMnu.html,
www.marcocirelli.net/DMnu.html.
- [27] A. E. Erkoca, M. H. Reno and I. Sarcevic, Phys. Rev. D **80**, 043514 (2009) [arXiv:0906.4364 [hep-ph]].
- [28] V. Barger, W. Y. Keung, G. Shaughnessy and A. Tregre, Phys. Rev. D **76** (2007) 095008 [arXiv:0708.1325 [hep-ph]].
- [29] S. Desai *et al.* [Super-Kamiokande Collaboration], Phys. Rev. D **70**, 083523 (2004) [Erratum-ibid. D **70**, 109901 (2004)] [arXiv:hep-ex/0404025].
- [30] R. Abbasi *et al.* [ICECUBE Collaboration], Phys. Rev. Lett. **102**, 201302 (2009) [arXiv:0902.2460 [astro-ph.CO]].
- [31] E. Resconi and f. t. I. Collaboration, Nucl. Instrum. Meth. A **602**, 7 (2009) [arXiv:0807.3891 [astro-ph]].
- [32] C. Wiebusch and f. t. I. Collaboration, arXiv:0907.2263 [astro-ph.IM].
- [33] W. F. McDonough, The Composition of the Earth (<http://quake.mit.edu/hilstgroup/CoreMantle/EarthCompo.pdf>), Chapter 1 in: Earthquake thermodynamics and phase transformations in Earth's interior (R. Teisseyre and E. Majewski, Eds.), Academic Press, 2000.
- [34] C. Delaunay, P. J. Fox and G. Perez, JHEP **0905**, 099 (2009) [arXiv:0812.3331 [hep-ph]].
- [35] A. Gould, Astrophys. J. **328**, 919 (1988).
- [36] E. Aprile, L. Baudis and f. t. X. Collaboration, arXiv:0902.4253 [astro-ph.IM].